2nd IFAC Workshop on Automatic Control in Offshore Oil and Gas Production,
May 27-29, 2015, Florianópolis, Brazil

Boundary control for stabilization of slugging oscillations

Gustavo A. de Andrade * **Daniel J. Pagano** *

* *Federal University of Santa Catarina, Automation and Systems Department, 88040-900, Florianópolis, SC, Brazil (e-mail: gustavo.artur@posgrad.ufsc.br, daniel.pagano@ufsc.br)*

Abstract: The problem of suppressing the slugging phenomenon is investigated. Industrial oil facilities such as gas-lifted wells and offshore production oil-risers are examples of systems where occurs such phenomenon. To study this problem, we consider that these systems are written as a set of 3×3 hyperbolic partial differential equations of balance laws, where the control variable appears at the boundary condition. By means of the characteristic coordinates approach, we deduce the stabilizing control law. The exponential stability of the equilibrium is proved by means of a Lyapunov stability analysis. Through simulation results, the method is shown effective in stabilizing the slugging phenomenon.

Keywords: boundary control, distributed parameter systems, flow control, partial differential equations, stabilization

1. INTRODUCTION

Slugging is a well-known two-phase flow regime which occurs in industrial oil facilities such as gas-lifted wells and offshore production oil-risers. This phenomenon is characterized by intermittent axial distribution of gas and liquid that leads to an oscillating flow pattern. Consequently, sudden variations of oil production due to changes in pressure and flow rates of liquid and gas may occur. Mature oil-fields, the increasing of gas-to-oil ratio and water fraction increases are probably the major cause of these unstable flow regimes.

A typical slugging bifurcation diagram, considering the outlet valve opening (production choke) as a bifurcation parameter, is shown in Fig. 1. As can be seen, a supercritical Hopf bifurcation takes place at the point HB_{sup}, giving rise to a stable limit cycle. As negative effects of this type of phenomenon, it can be mentioned the oil production detriment and several issues concerning safety of operations on the surface equipment, which can provoke several undesired effects as deteriorating the separation quality and level overflow in the multiphase flow separator (Stasiak et al., 2012; Di Meglio et al., 2012a).

The fluid flow regime stabilization in industrial oil facilities has the potential for immense economical benefits (Storkaas and Skogestad, 2007), since the system can operate with a larger outlet valve opening, and the flow stabilization minimize the problems on the separator. Many methodologies have been developed to avoid the undesirable slugging phenomenon, between them, the active control of the outlet valve has been shown a promising method to suppress these oscillations (Godhavn et al., 2003).

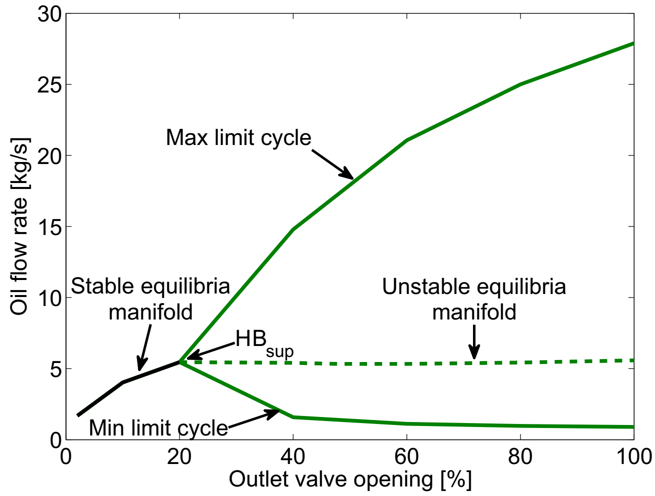

Fig. 1. Typical bifurcation diagram considering the outlet valve opening as the bifurcation parameter. A stable limit cycle undergoes from a supercritical Hopf Bifurcation (HB_{sup}).

However, slug flow stabilization via active control is not trivial. These systems are characterized by partial differential equations (PDEs), boundary actuator, nonlinearities and uncertainties. Therefore, simple controllers cannot operate effectively in the whole operating point due to the complex dynamic involved in slug flow. Some advanced control techniques reported in literature to deal with this control problem can be found in Storkaas and Skogestad (2007); Stasiak et al. (2012); Pagano et al. (2009); Di Meglio et al. (2012b); Godhavn et al. (2003). These controllers use mainly upstream pressure sensors (a sensor located at the bottom of the pipe) in the feedback-loop to stabilize the flow by outlet valve actuation. Even further, all these results are based on simplified lumped parameter models, and most of them are not based on a rigorous first

⋆ Gustavo Artur de Andrade thanks the financial support given by the CNPq.

principles dynamic model. The higher model complexity is probably the main reason why model based controllers are still scarce in literature.

In this paper, we propose a feedback controller to stabilize the slugging oscillations in multiphase flow based on an infinite dimensional 3×3 linear system, where the control variable appears at the boundary condition. Few results in literature address this control problem from this point of view. As far as we know, the slug flow stabilization using boundary control theory has only been previously investigated in Di Meglio et al. (2012c), where a full-state feedback law based on a 3×3 linearized quasilinear hyperbolic model was proposed. This control system uses a backstepping transformation to find new variables for which a Lyapunov function can be constructed, achieving exponential stability for the $\mathscr{L}^2(0, L)$-norm.

Our proposal is based on the ideas of Diagne et al. (2012); Bastin et al. (2008), where a proportional feedback control law is presented and the closed-loop stability is demonstrated using characteristic coordinates along with an appropriate Lyapunov function. The control system is based in a similar linearized PDE model of Di Meglio et al. (2012a). However, in our model the friction against the pipe walls is considered and a homogeneous model for the two-phase flow is used. The proposed control strategy was tested via numerical simulations on the nonlinear PDE model to show its relevance.

The paper is organized as follows. In Section 2, we describe the slugging model. In Section 3, the Lyapunov stability analysis of the proposed controller is shown. The control design is shown in Section 4. We illustrate the simulation results in Section 5. Conclusions are given in Section 6.

2. THE SLUGGING MODEL

In this work, a PDE model is used to describe the slugging phenomenon in industrial oil facilities. The model is similar to that proposed by Di Meglio et al. (2012a), but the friction against the pipe walls is considered and a homogeneous model for the two-phase flow is used. Moreover, it is assumed constant temperature along the pipe, incompressible oil, and no mass transfer between the gas and liquid phase. In this context, the PDEs that describe the system behavior are given by

$$\frac{\partial \alpha_g \rho_g}{\partial t} + \frac{1}{A}\frac{\partial q_g}{\partial z} = 0, \tag{1}$$

$$\frac{\partial \alpha_l \rho_l}{\partial t} + \frac{1}{A}\frac{\partial q_l}{\partial z} = 0, \tag{2}$$

$$\frac{\partial \rho_m v_m}{\partial t} + \frac{\partial P + \rho_m v_m^2}{\partial z} = -\frac{f}{2d}\rho_m v_m^2 - \rho_m g sin\theta(z), \tag{3}$$

where, for $k = g$ or l, α_k denotes the volume fraction of phase k, ρ_k its density and q_k its flow rate. The pressure is denoted by P, ρ_m is the density of the mixture, v_m is the velocity of the mixture, f accounts for the friction factor, d is the pipe diameter and A its cross-section area, and $\theta(z)$ is the inclination of the pipe. The time variable is $t \in [0, +\infty)$ and $z \in [0, L]$ is the space variable, where L is the length of the pipe.

Besides the PDE model (1)-(3), the following algebraic equations are used for system closure:

$$\alpha_g + \alpha_l = 1, \tag{4}$$

$$\rho_m = \alpha_g \rho_g + \alpha_l \rho_l, \tag{5}$$

$$P = \frac{\rho_g R T}{M}, \tag{6}$$

$$x = \frac{\alpha_g \rho_g}{\alpha_g \rho_g + \alpha_l \rho_l}, \tag{7}$$

where R is the specific gas constant, M is the gas molar weight, x is the gas mass fraction, and T is the temperature.

Regarding the boundary conditions, they are given at both ends of the pipe. At the bottom, two boundary conditions are given: one for the liquid flow rate, assuming that it is linearly depend on the pressure drop between the pipe and the oil reservoir, and other boundary condition for the gas flow rate, assumed to be constant. They are expressed as

$$q_l(t, 0) = PI[P_r - P(t, 0)], \tag{8}$$

$$q_g(t, 0) = q_g, \tag{9}$$

where q_l is the liquid flow rate, q_g is the gas flow rate, PI is a constant coefficient called productivity index and P_r is the pressure in the reservoir, assumed to be constant.

At the top, the total flow rate, $q_t = q_l + q_g$, is assumed to be governed by a valve equation of given by

$$q_t(t, L) = C_{out} Z(t) \sqrt{\rho_m(t, L)(P(t, L) - P_s)}, \tag{10}$$

where P_s is the pressure in the separator, C_{out} is a valve constant and $Z(t)$ is the valve opening, which is the manipulated variable.

2.1 Formulating the Slugging Model as a Quasilinear System

Combining the equations (1)-(3), the static relations (4)-(7), and considering the following state vector

$$\mathbf{u} = [\, u_1 \;\; u_2 \;\; u_3 \,]^T = \left[\, P \;\; q_t \;\; \frac{\alpha_g \rho_g}{\alpha_g \rho_g + \alpha_l \rho_l} \,\right]^T,$$

it is possible to rewrite the system in quasilinear form

$$\frac{\partial \mathbf{u}}{\partial t} + F(\mathbf{u}, z)\frac{\partial \mathbf{u}}{\partial z} = S(\mathbf{u}, z). \tag{11}$$

The expressions of the matrices $F(\mathbf{u}, z)$ and $S(\mathbf{u}, z)$ are given in the Appendix A.

2.2 Steady-state and linearized system

The steady-state solution for system (11) is a constant solution $\mathbf{u}(t, z) = \mathbf{u}^*$, $\forall t \in [0, +\infty)$, $\forall z \in [0, L]$, satisfying the boundary conditions (8)-(10) and the condition

$$f u_3^2 \frac{(1-u_3^*)\left((1-u_3^*)M^2 {u_1^*}^2 + 2MRT\rho_l u_3^* u_1^*\right) + R^2 T^2 \rho_l^2 {u_3^*}^2}{2AMd\rho_l u_1^*((1-u_3^*)M u_1^* + RT\rho_l u_3^*)} = - \frac{AM\rho_l}{(1-u_3^*)M u_1^* + RT\rho_l u_3^*} g \sin\theta(z). \tag{12}$$

In order to linearize the system (11) and its boundary conditions (8)-(10), we define the deviations of the states $u_1(t, z)$, $u_2(t, z)$ and $u_3(t, z)$ with respect to the steady-states u_1^*, u_2^* and u_3^* by

$$\delta u_1(t, z) \triangleq u_1(t, z) - u_1^*,$$

$$\delta u_2(t, z) \triangleq u_2(t, z) - u_2^*,$$

$$\delta u_3(t, z) \triangleq u_3(t, z) - u_3^*.$$

Then, the linearized quasilinear model (11) around the steady-state (see Bastin et al. (2008)) is described by

$$\frac{\partial \delta \mathbf{u}}{\partial t} + F(\mathbf{u}^*)\frac{\partial \delta \mathbf{u}}{\partial z} + \tilde{S}(\mathbf{u}^*)\delta \mathbf{u} = 0, \tag{13}$$

where

$$\delta \mathbf{u} \triangleq [\, \delta u_1 \;\; \delta u_2 \;\; \delta u_3 \,]^T,$$
$$\mathbf{u}^* \triangleq [\, u_1^* \;\; u_2^* \;\; u_3^* \,]^T,$$
$$\tilde{S}(\mathbf{u}^*) \triangleq \left[\, \tfrac{\partial S}{\partial u_1}(\mathbf{u}^*) \;\; \tfrac{\partial S}{\partial u_2}(\mathbf{u}^*) \;\; \tfrac{\partial S}{\partial u_3}(\mathbf{u}^*) \,\right].$$

Let $q_l = (1 - u_3)u_2$. Then, the linearized boundary condition (8) results in the following expression:

$$PI\delta u_1(t,0) + (1 - u_3^*)\delta u_2(t,0) - u_2^*\delta u_3(t,0) = 0. \tag{14}$$

Similarly, consider $q_g = u_3 u_2$. Then, the linearized boundary condition (9) is given by

$$u_3^*\delta u_2(t,0) + u_2^*\delta u_3(t,0) = 0. \tag{15}$$

Finally, the linearized boundary condition (10) is expressed as

$$\delta u_2(t,L) = K_{u_1}\delta u_1(t,L) + K_{u_3}\delta u_3(t,L) + K_z \delta z(t), \tag{16}$$

where $\delta z(t) = Z(t) - Z^*$, being Z^* the choke opening steady state value, and

$$K_{u_3} = -\frac{(\rho_L RT - u_1^*)u_2^*}{2(\rho_L RT u_3^* + (1 - u_3^*)u_1^*)},$$
$$K_{u_1} = \frac{\rho_L u_1^*(2\rho_L RT u_3^* + (1 - u_3^*)u_1^*) - P_s\rho_L^2 RT u_3^*}{2(\rho_L RT u_3^* + (1 - u_3^*)u_1^*)} \times \frac{u_2^*}{\rho_L u_1^*(u_1^* - P_s)},$$
$$K_z = C_{out}\sqrt{\frac{\rho_L u_1^*}{\rho_L RT u_3^* + (1 - u_3^*)u_1^*}(u_1^* - P_s)}.$$

2.3 Model in terms of characteristic coordinates

In this section, we transform the system (13) into the so-called characteristic form by using the characteristic coordinates (Bastin et al., 2008).

To this aim, let us consider the following change of coordinates:

$$R_1(t,z) = \delta u_2(t,z) + a\delta u_3(t,z) + b\delta u_1(t,z), \tag{17}$$
$$R_2(t,z) = \delta u_2(t,z) + a\delta u_3(t,z) - b\delta u_1(t,z), \tag{18}$$
$$R_3(t,z) = \delta u_3(t,z), \tag{19}$$

where

$$a = \frac{RT\rho_l u_2 - M u_1 u_2}{(1-u_3)M u_1 + RT\rho_l u_3},$$
$$b = \rho_l \frac{A u_1 \sqrt{M^3 RT u_3 - MRT u_3 u_2}}{M u_1((1-u_3)M u_1 RT\rho_l u_3)}.$$

With these new coordinates, the system (13) is rewritten in the following form:

$$\frac{\partial \mathbf{R}}{\partial t} + \Lambda\frac{\partial \mathbf{R}}{\partial z} + \Sigma\mathbf{R} = 0 \tag{20}$$

with

$$\mathbf{R} \triangleq [\, R_1(t,z) \;\; R_2(t,z) \;\; R_3(t,z) \,]^T,$$

and Λ is the matrix with the transport speeds, given by

$$\Lambda = \begin{bmatrix} \lambda_1 & 0 & 0 \\ 0 & -|\lambda_2| & 0 \\ 0 & 0 & \lambda_3 \end{bmatrix} \tag{21}$$

The expressions of the transport speeds are shown in Eq. (A.3), and they satisfy the following inequalities:

$$\lambda_2 < 0 < \lambda_3 < \lambda_1$$

The expression for Σ is complicated to be written in details. Then, to save space, we express its structure as

$$\Sigma = \begin{bmatrix} \sigma_{1,1} & \sigma_{1,2} & \sigma_{1,3} \\ \sigma_{2,1} & \sigma_{2,2} & \sigma_{2,3} \\ 0 & 0 & 0 \end{bmatrix} \tag{22}$$

Note that the last line of Σ is filled with 0. This occurs because the state variable $u_3(t, z)$ is a Riemann invariant (Di Meglio et al., 2012c). This structure is also preserved by the transformation shown in this section.

Several numerical tests performed for the system considered in this work (see Section 5 for details about the system geometry) have shown that the following inequalities hold:

$$\sigma_{1,3} \equiv \sigma_{2,3} < 0 < \sigma_{1,1} \equiv \sigma_{2,1} < \sigma_{1,2} \equiv \sigma_{2,2}$$

Typical values are $\sigma_{1,3} \equiv \sigma_{2,3} \approx -425$, $\sigma_{1,2} \equiv \sigma_{2,2} \approx 15224$, and $\sigma_{1,3} \equiv \sigma_{2,3} \approx 0.4$.

Finally, the boundary conditions (14)-(16), in characteristic coordinates, are expressed as

$$R_1(t,0) - \psi R_2(t,0) = 0, \tag{23}$$
$$R_2(t,L) + k_1 R_1(t,L) + k_2 R_2(t,0) + k_3 R_3(t,L) = 0, \tag{24}$$
$$R_3(t,0) - \varphi R_2(t,0) = 0, \tag{25}$$

or in matrix form

$$\begin{bmatrix} R_1(t,0) \\ R_2(t,L) \\ R_3(t,0) \end{bmatrix} = \underbrace{\begin{bmatrix} 0 & \psi & 0 \\ -k_1 & -k_2 & -k_3 \\ 0 & \varphi & 0 \end{bmatrix}}_{\mathbf{K}} \begin{bmatrix} R_1(t,L) \\ R_2(t,0) \\ R_3(t,L) \end{bmatrix}, \tag{26}$$

where

$$\varphi = \frac{PI u_3^*}{PIa u_3^* - 2u_3^* u_2^* - PIb u_2^*},$$
$$\psi = \frac{u_3^* + 2bu_2^*}{u_3^* - 2bu_2^*},$$

and k_i, $i = 1, ..., 3$ are constant design parameters that have to be tuned to guarantee the stability of the linear system (13), as will be shown in the next section.

The change of coordinates (17)-(19) is inverted as follows:

$$\delta u_1(t,z) = \frac{R_1(t,z) + R_2(t,z) - 2aR_3(t,z)}{2}, \tag{27}$$
$$\delta u_2(t,z) = \frac{R_1(t,z) - R_2(t,z)}{2b}. \tag{28}$$
$$\delta u_3(t,z) = R_3(t,z). \tag{29}$$

3. STABILITY ANALYSIS

In characteristic coordinates, the control problem can be restated as the problem of determining the control action in such a way that the solution $R_1(t,z)$, $R_2(t,z)$, $R_3(t,z)$ converge towards zero (Coron et al., 2007). We now investigate the stabilization of the linearized system (13) imposing the boundary control (24).

We introduce the following candidate Lyapunov function (Bastin et al., 2008):

$$V(t) = \int_0^L R_1^2(t,z)p_1 \exp(-\mu z)dz + \int_0^L R_2^2(t,z)p_2 \exp(\mu z)dz + \int_0^L R_3^2(t,z)p_3 \exp(-\mu z)dz \quad (30)$$

with $\mu > 0$, $p_i > 0$, $i = 1, ..., 3$ yet to be defined. Also, we define the following notations:

$$R_1(0) \triangleq R_1(t,0) \qquad R_1(L) \triangleq R_1(t,L)$$
$$R_2(0) \triangleq R_2(t,0) \qquad R_2(L) \triangleq R_2(t,L)$$
$$R_3(0) \triangleq R_3(t,0) \qquad R_3(L) \triangleq R_3(t,L)$$

Differentiating $V(t)$ and integrating by parts one obtains

$$\dot{V} = \dot{V}_1 + \dot{V}_2, \quad (31)$$

where

$$\dot{V}_1 \triangleq -\left[\left(R_1^2(t,z)p_1\lambda_1 + R_3^2(t,z)p_3\lambda_2\right)\exp(-\mu z)\right]_0^L + \left[R_2^2(t,z)p_2|\lambda_2|\exp(\mu z)\right]_0^L, \quad (32)$$

and the expression for $\dot{V}_2$ is shown in Eq. (33).

If the function $\dot{V}$ is negative definite, then the system (20) is exponentially stable (Khalil, 2002). We now investigate the two terms of (31) successively in order to prove stability.

The analysis of (32) (using the boundary conditions (23)-(25)) gives

$$\dot{V}_1 = -\left(R_2(0)^2 p_2|\lambda_2| + R_1(L)^2\lambda_1 p_1 \exp(-\mu L) + R_3(L)^2\lambda_3 p_3 \exp(-\mu L)\right) + \varphi^2 R_2^2(0)p_1\lambda_1 + \psi^2 R_2^2(0)p_2\lambda_2 + \left(k_3R_3(0) + k_1R_1(L) + k_2R_2(L)\right)^2 p_3|\lambda_3|\exp(\mu L). \quad (34)$$

As shown in Diagne et al. (2012), $\dot{V}_1(t)$ is a negative definite quadratic form with respect to $\mathbf{R}$ $\forall t \geq 0$ along the solutions of the linearized system (20) if the norm for the matrix $\mathbf{K}$

$$\rho(\mathbf{K}) \triangleq \left\{||\Delta\mathbf{K}\Delta^{-1}||, \Delta \in \mathscr{S}\right\}, \quad (35)$$

where $||\cdot||$ denotes the matrix 2-norm, and the set $\mathscr{S}$ is defined as

$$\mathscr{S} \triangleq \left\{\Delta = \mathrm{diag}\{\sqrt{p_1\lambda_1}, \sqrt{p_2|\lambda_2|}, \sqrt{p_3\lambda_3}\}\right\}, \quad (36)$$

satisfies

$$\rho(\mathbf{K}) < 1. \quad (37)$$

Therefore, using (26) and the inequality (37) we obtain

$$\left\|\begin{bmatrix} 0 & \psi\sqrt{\dfrac{\lambda_1 p_1}{|\lambda_2|p_2}} & 0 \\ -k_1\sqrt{\dfrac{|\lambda_2|p_2}{\lambda_1 p_1}} & -k_2 & -k_3\sqrt{\dfrac{|\lambda_2|p_2}{p_3\lambda_3}} \\ 0 & \varphi\sqrt{\dfrac{\lambda_3 p_3}{|\lambda_2|p_2}} & 0 \end{bmatrix}\right\| < 1, \quad (38)$$

it follows that $\dot{V}_1$ is negative definite.

A sufficient condition for $\dot{V}_2$ be negative definite is that the principal minors of Q are strictly positive. Evaluating such operation we obtain the following inequalities:

$$\mu\lambda_1 + 2\sigma_{11} > 0 \quad (39)$$
$$\mu|\lambda_2| + 2\sigma_{22} > 0 \quad (40)$$
$$(\mu\lambda_1 + 2\sigma_{11})(\mu|\lambda_2| + 2\sigma_{22})p_1p_2 - (\sigma_{21}p_2\exp(\mu z) + \sigma_{12}p_1\exp(-\mu z))^2 > 0 \quad (41)$$
$$\mu\lambda_3 p_3 \exp(-\mu z)\left[(\mu\lambda_1 + 2\sigma_{11})(\mu|\lambda_2| + 2\sigma_{22})p_1p_2 - (\sigma_{21}p_2\exp(\mu z) + \sigma_{12}p_1\exp(\mu z))^2\right] - \sigma_{23}\exp(\mu z)\times \left[(\mu\lambda_1 + 2\sigma_{11})\sigma_{32}p_1p_2 - (\sigma_{21}p_2\exp(\mu z) + \sigma_{12}p_1\exp(-\mu z))\sigma_{13}p_1\exp(-\mu z) + \sigma_{13}p_1\exp(-\mu z)\right] + \sigma_{13}p_1\exp(-\mu z)\left[(\sigma_{21}p_2\exp(\mu z) + \sigma_{12}p_1\exp(-\mu z))\times \sigma_{23}p_2\exp(\mu z) - (\mu|\lambda_2| + 2\sigma_{22})p_1p_2\right] > 0 \quad (42)$$

Conditions (39)-(40) are satisfied for any $\mu \geq 0$. Condition (41) is satisfied for sufficiently small $\mu > 0$ if the parameters p_1, p_2 are selected such that $\sigma_{12}p_1 = \sigma_{21}p_2$, as shown in Bastin et al. (2008). Under this condition, the term $(\sigma_{21}p_2\exp(-\mu x) + \sigma_{12}p_1\exp(\mu x))^2$ is maximum either at $x = 0$ or at $x = L$. For $x = 0$, we have

$$(\mu\lambda_1 + \sigma_{11})(\mu|\lambda_2| + 2\sigma_{22})p_1p_2 - (\sigma_{21}p_2 + \sigma_{32}p_3)^2 > 0$$
$$= \mu^2\lambda_1|\lambda_2|p_1p_2 + \mu p_1p_2\left[2\sigma_{22} + 2\sigma_{11}|\lambda_2|\right] > 0$$

for any $\mu > 0$. On the other hand, for $x = L$ we have

$$(\mu\lambda_1 + \sigma_{11})(\mu|\lambda_2| + 2\sigma_{22})p_1p_2 - (\sigma_{21}p_2\exp(\mu L) + \sigma_{32}p_3\exp(\mu L))^2 > 0$$
$$= \mu^2\lambda_1|\lambda_2|p_1p_2 + \mu p_1p_2\left[2\sigma_{22} + 2\sigma_{11}|\lambda_2|\right] - (\sigma_{11}p_2\exp(-\mu L) - \sigma_{22}p_3\exp(\mu L))^2 > 0$$

for $\mu > 0$ sufficiently small.

Finally, inequality (42) is satisfied for a sufficiently large p_3. It follows that there exist $\alpha > 0$ such that

$$\dot{V}_2 < -\alpha V \Longrightarrow \dot{V} = \dot{V}_1 + \dot{V}_2 \leq -\alpha V \qquad \forall \mathbf{R} \neq 0. \quad (43)$$

Hence, V is a Lyapunov function along the solutions of the linearized slugging model and its solutions exponentially converge to $\mathbf{0}$ in $\mathscr{L}^2(0,L)$-norm.

We have to stress that the Lyapunov function used in this section to show the stability of the linear system cannot be used to analyze the local stability of the nonlinear case. To this aim, an augmented Lyapunov function must be used to prove convergence in $H^2(0,L)$-norm. This proof is much more complicated than the linear case shown in this section and it is out of scope of this paper. The interested reader can see Coron et al. (2007); Bastin et al. (2008) for more details.

4. DESIGN OF THE CONTROL LAW

In the previous section, we have seen that the system stability is guaranteed if the feedback control law (24) holds. Therefore, in this section we shall present how the explicit expression of the control law can be obtained using the boundary condition (16).

We introduce the following notations:

$$\delta u_1(L) \triangleq \delta u_1(t,L) \qquad \delta u_1(0) \triangleq \delta u_1(t,0)$$
$$\delta u_2(L) \triangleq \delta u_2(t,L) \qquad \delta u_2(0) \triangleq \delta u_2(t,0)$$
$$\delta u_3(L) \triangleq \delta u_3(t,L) \qquad \delta u_3(0) \triangleq \delta u_3(t,0)$$

Using the definition of the Riemann coordinates (17)-(19) the boundary condition (24) is rewritten as

$$\dot{V}_2 \triangleq -\int_0^L \mathbf{R}^T \underbrace{\begin{bmatrix} (\mu\lambda_1 + 2\sigma_{11})p_1 \exp(-\mu z) & \sigma_{21}p_2 \exp(\mu z) + \sigma_{12}p_1 \exp(-\mu z) & \sigma_{13}p_1 \exp(-\mu z) \\ \sigma_{21}p_2 \exp(\mu z) + \sigma_{12}p_1 \exp(-\mu z) & (\mu|\lambda_2| + 2\sigma_{22})p_2 \exp(\mu z) & \sigma_{23}p_2 \exp(\mu z) \\ \sigma_{13}p_1 \exp(-\mu z) & \sigma_{23}p_2 \exp(\mu z) & \mu\lambda_3 p_3 \exp(-\mu z) \end{bmatrix}}_{Q} \mathbf{R} \quad (33)$$

$$\delta u_3(L)(a + k_1 a + k_3) - \delta u_1(k_1 b - b) + \delta u_3(L)(1 + k_1) + k_2(\delta u_2(0) + a\delta u_3(0) - b\delta u_1(0)) = 0. \quad (44)$$

Then, by eliminating $\delta u_3(L)$ between (16) and (44), and eliminating $\delta u_2(0)$ and $\delta u_3(0)$ between (14), (15) and (44), we get the following expression for the control law

$$Z(t) = Z^* + K_{p_{u_2}}\delta u_2(L) + K_{p_{u_1}}\delta u_1(L) + K_{p_0}\delta u_1(0), \quad (45)$$

where

$$K_{p_{u_2}} = \frac{k_3 + K_{u_3} + a + k_1 a + k_1 K_{u_3}}{K_z\,(a + k_1 a + k_3)},$$

$$K_{p_{u_1}} = \frac{K_{u3}}{K_z(a+k_1a+k_3)}\left(k_1 b - b - \frac{K_{u_1}}{K_{u_3}}(a + k_1 a + k_3)\right),$$

$$K_{p_0} = \frac{K_{u_3}k_2\,(PI(au_3^*/u_2^* - 1) - b)}{K_z\,(a + k_1 a + k_3)}.$$

It must be noted that the feedback control law (45) need measurements of pressure at the outlet valve, the bottom pressure and total flow-rate measurement through the outlet valve. For the simulations results shown Section 5, we consider that all these variables are being measured. In some real cases this is not true. Therefore, the use of a state observer together with the control law is probably the best option in these cases.

5. SIMULATION RESULTS

This section shows the simulation results obtained when using the proposed controller to stabilize the quasilinear model (11). We consider a 2500 meter long vertical well with reservoir pressure $P_r = 180$ bar and separator pressure $P_s = 10$ bar. The space was divided in N sections and the space derivatives were written using a finite difference scheme. An ODE solver was used to obtain the solution.

In Fig. 2 is shown an open loop simulation of the quasilinear system (11). The simulation starts with the production choke opened to $Z = 100\%$ and then after $t = 8$ h the production choke is closed to $Z = 50\%$ and to $Z = 20\%$ after more 8 hours. The oscillations have a period around of 50 minutes. For this case study, the supercritical Hopf bifurcation point, HB_{sup} take place at a valve opening $Z(t) = 22\%$ (this value was found by performing several simulations for different valve openings). The corresponding open-loop bifurcation diagram for the valve opening is shown in Fig. 1.

In Fig. 3 the results obtained with the control technique proposed in this paper are shown. The operating point was chosen to be $Z^* = 48\%$. The steady-state values of $u_2^*(0)$, $u_2^*(L)$ and $u_3^*(L)$, necessary for the control law, can be obtained by computing the steady-state model (11) in such operating point. The controller gains were chosen to be $k_1 = -0.5$, $k_2 = 2.3$ and $k_3 = 300$. These parameters were found after several simulations. At $t = 3.3$ h the control

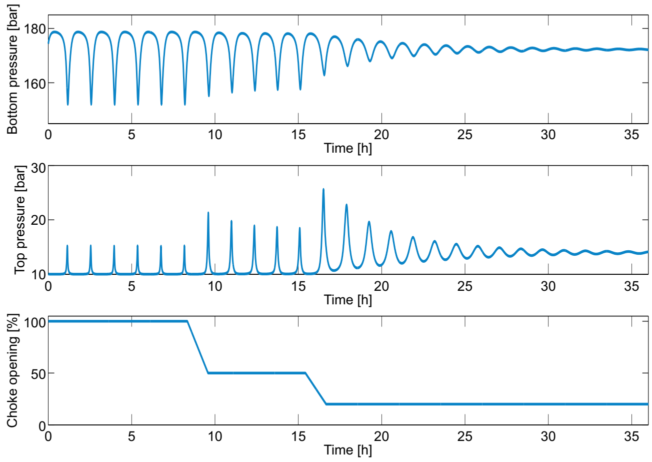

Fig. 2. Botton and top pressure for different choke opening values.

was switched on. It can be noted that the oscillations are suppressed and the system remains in the desired operating point. At $t = 15$ h the control was switched off and as expected, the system comes back to the oscillatory regime.

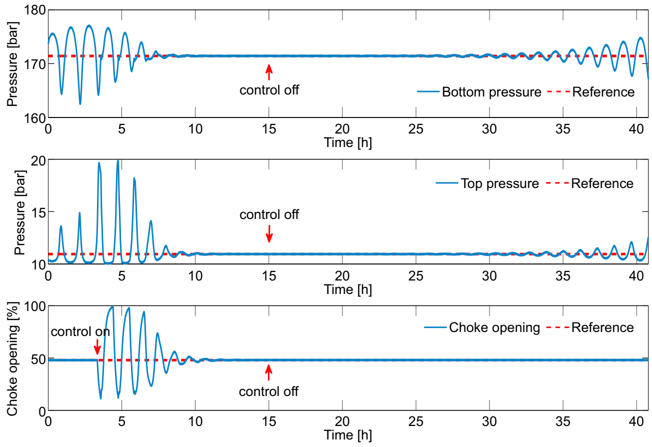

Fig. 3. Bottom and top pressure, and choke opening with the proposed control law. At $t = 3.3$ h the control was switched on and at $t = 15$ h the control was again switched off.

6. CONCLUSION

In this paper, we have proposed a boundary control to stabilize slugging flow. The control law has a simple structure and is needed measurements only at both system boundaries. Moreover, as shown in Section 3, the linearized system has exponential stability of the origin in $\mathscr{L}^2(0, L)$-norm with the proposed controller.

Although the exponential stability of the proposed control law in the nonlinear system has not been shown, the simulations results are showing to be promising. The extension to the nonlinear case can be a direction of future work.

The simulations results shown in this paper consider the inlet of gas constant. From a practical point of view, it should be considered influxes of gas. The control performance for this case is under investigation.

Moreover, we have to stress that in our simulations it was considered that the pressure is measured at the bottom of the pipe, which in some cases it is not a realistic scenario. The use of a state observer together with the control law is probably the best option in these cases. The recent work of Castillo et al. (2013) may be a good approach to address this issue. This is another direction for further research.

REFERENCES

Bastin, G., Coron, J.M., and d'Andréa Novel, B. (2008). Boundary feedback control and lyapunov stability analysis for physical networks of 2×2 hyperbolic balance laws. In *Proceedings of the 47th IEEE Conference on Decision and Control*, 1454–1458.

Castillo, F., Witrant, E., Prieur, C., and Dugard, L. (2013). Boundary observers for linear and quasilinear hyperbolic systems with application to flow control. *Automatica*, 49(11), 3180–3188.

Coron, J.M., d'Andréa Novel, B., and Bastin, G. (2007). A strict Lyapunov function for boundary control of hyperbolic systems of conservation laws. *IEEE Transactions on Automatic Control*, 52(1), 2–11.

Di Meglio, F., Kaasa, G.O., Petit, N., and Alstad, V. (2012a). Slugging in multiphase flow as a mixed initial-boundary value problem for a quasilinear hyperbolic system. In *Proceedings of the American Control Conference 2012*, 3589–3596.

Di Meglio, F., Petit, N., Alstad, V., and Kaasa, G.O. (2012b). Stabilization of slugging in oil production facilities with or without upstream pressure sensors. *Journal of Process Control*, 22(4), 809–822.

Di Meglio, F., Vazquez, R., Krstic, M., and Petit, N. (2012c). Backstepping stabilization of an underactuated 3×3 linear hyperbolic system of fluid flow equation. In *Proceedings of the American Control Conference 2012*, 3365–3370.

Diagne, A., Bastin, G., and Coron, J.M. (2012). Lyapunov exponential stability of 1-D linear hyperbolic systems of balance laws. *Automatica*, 48(1), 109–114.

Godhavn, J., Fard, M.P., and Cuchs, P.H. (2003). New slug control strategies, tuning rules and experiments results. *Journal of Process Control*, 15, 547–557.

Khalil, H.K. (2002). *Nonlinear systems.* Prentice Hall, Upper Saddle River, USA.

Pagano, D.J., Plucenio, A., and Traple, A. (2009). Slug-flow control in submarine oil-risers using SMC strategies. In *Proceedings of the 7th IFAC Symposium on Advanced Chemical Control Systems*, 566–571.

Stasiak, M.E., Pagano, D.J., and Plucenio, A. (2012). A new discrete slug-flow controller for production pipeline risers. In *Proceedings of the 1th IFAC Workshop on Automatic Control in Offshore Oil and Gas Production*, 122–127.

Storkaas, E. and Skogestad, S. (2007). Controllability analysis of two-phase pipeline-riser systems at riser slugging conditions. *Control Engineering Practice*, 15(5), 567–581.

Appendix A

The matrices $F(\mathbf{u}, z)$ and $S(\mathbf{u}, z)$ corresponding to the quasilinear system (11), and the eigenvalues of $F(\mathbf{u}, z)$ are given by the following expressions:

$$F(\mathbf{u}, z) = \begin{bmatrix} 0 & \frac{((1-u_3)Mu_1+RT\rho_l u_3)^2}{AMRT\rho_l^2 u_3} & -\frac{u_2(Mu_1-RT\rho_l)((1-u_3)Mu_1+RT\rho_l u_3)}{AMRT\rho_l^2 u_3} \\ A - \frac{RTu_3u_2^2}{AMu_1^2} & 2\frac{(1-u_3)Mu_1u_2+RT\rho_l u_3 u_2}{AM\rho_l u_1} & \frac{RT\rho_l u_2^2 - Mu_1u_2}{AM\rho_l u_1} \\ 0 & 0 & u_2\frac{(1-u_3)Mu_1+RT\rho_l u_3}{AM\rho_l u_1} \end{bmatrix} \tag{A.1}$$

$$S(\mathbf{u}, z) = \begin{bmatrix} 0 \\ \frac{AM\rho_l}{(1-u_3)Mu_1+RT\rho_l u_3} g\sin\theta(z) + fu_2^2\frac{(1-u_3)\left((1-u_3)M^2u_1^2+2MRT\rho_l u_3 u_1\right)+R^2T^2\rho_l^2u_3^2}{2AMd\rho_l u_1((1-u_3)Mu_1+RT\rho_l u_3)} \\ 0 \end{bmatrix} \tag{A.2}$$

$$\begin{bmatrix} \lambda_1 \\ \lambda_2 \\ \lambda_3 \end{bmatrix} = \begin{bmatrix} \frac{\left((1-u_3)AMu_1^2+ART\rho_l u_3 u_1\right)\sqrt{M^3RTu_3}}{AM^2RT\rho_l u_3 u_1} + \frac{u_2(1-u_3)}{A\rho_l} + \frac{Ru_3u_2}{AMu_1} \\ -\frac{\left((1-u_3)AMu_1^2+ART\rho_l u_3 u_1\right)\sqrt{M^3RTu_3}}{AM^2RT\rho_l u_3 u_1} + \frac{u_2(1-u_3)}{A\rho_l} + \frac{Ru_3u_2}{AMu_1} \\ u_2\frac{(1-u_3)Mu_1+RT\rho_l u_3}{AM\rho_l u_1} \end{bmatrix} \tag{A.3}$$

